Miscibility, Specific Interactions, and Spherulite Growth Rates of Binary Poly(acetoxystyrene)/Poly(ethylene oxide) Blends

Shiao-Wei Kuo,[†] Wu-Jang Huang,[‡] Chih-Feng Huang,[†] Shih-Chi Chan,[†] and Feng-Chih Chang*[,†]

Institute of Applied Chemistry, National Chiao Tung University, Hsin Chu, Taiwan, and Department of Environmental Science and Engineering, National Ping-Tung University of Science and Technology, Ping-Tun, Taiwan

Received September 22, 2003; Revised Manuscript Received March 24, 2004

ABSTRACT: The binary poly(acetoxystyrene)/poly(ethylene oxide) (PAS/PEO) blend system is fully miscible, as evidenced by a single glass transition temperature over a full range of compositions when analyzed by differential scanning calorimetry analysis, as a result of weak C−H···O hydrogen-bonding interactions between the carbonyl groups of PAS and the methylene groups of PEO. One- and two-dimensional correlation spectroscopies provide positive evidence for this specific interaction between the two polymers. In addition, a negative polymer−polymer interaction parameter "χ_{12}" was calculated using the Flory−Huggins equation based on the melting depression of PEO. The presence of an amorphous PAS phase results in a reduction in the spherulite growth rate of PEO. Both the values of nucleation constant and the surface free energy of chain folding of PEO decrease with increasing PAS content, which indicates that the crystallization ability of PEO increases correspondingly.

Introduction

The study of the miscibility behavior of polymer blends is critical to the design of new polymeric materials with interesting properties. Most pairs of polymers are immiscible, however, because of only a small gain in entropy blending. To enhance the formation of a one-phase miscible system in polymer blends, it is essential to ensure that favorable specific intermolecular interactions exist between the two base components of the blend. Ideally, one polymer should possess donor sites and the other possesses acceptor sites on their respective chains. The most commonly observed interactions are of the acid−base type, i.e., hydrogen bonding,[1] dipole−dipole, and charge-transfer interactions.

Poly(ethylene oxide) (PEO) is a highly crystalline polymer that is miscible with several amorphous polymers, such as phenoxy,[2,3] poly(acrylic acid),[4−7] poly(vinyl alcohol),[8] poly(vinylphenol),[9,10] and phenolic resin[11,12] through the formation of strong hydrogen bonds. In addition, blends of PEO with many weakly interacting polymers, such as poly(methyl methacrylate) (PMMA),[13,14] poly(vinyl acetate),[15,16] and poly(vinylpyrrolidone),[17] are also fully miscible. Miscible blends of PEO with PMMA have been widely studied in the literature, with analyses ranging from melting point depressions,[18] changes in glass transition temperatures,[19] and measurements of spherulite growth and crystallization rates.[20] The results indicate that the blend components are miscible in the melt and in the amorphous phase. PEO can act as a Lewis base since the oxygen atom bears a partial negative charge, while the carbonyl carbon atom of PMMA has a partial positive charge. No strong hydrogen bonding is expected between PEO and PMMA. Russell et al.[21] applied the neutron scattering method to determine the interaction parameter of PEO/PMMA blends and found a small negative value, which suggests that very weak interactions exist between PEO and PMMA. The existence of very weak specific interaction between PEO and PMMA was also confirmed by vibrational spectroscopy.[22]

In this study, we have investigated the miscibility of binary blends of semicrystalline PEO with amorphous poly(acetoxystyrene) (PAS) by differential scanning calorimetry (DSC), Fourier transform infrared spectroscopy (FTIR), and optical microscopy (OM). FTIR spectroscopy has been commonly employed to identify the interactions between different polymeric components, such as blends featuring strong hydrogen-bonding interactions.[1,23] The observed significant shifts in certain infrared bands can be attributed to strong intermolecular hydrogen bonding between the hydroxyl group of donor polymers, such as poly(vinylphenol), phenolic resin, and phenoxy and acceptor polymers, including polyether, polyester, poly(acrylate), and poly(vinylpyridine).[1,23] Relatively fewer discussion, however, concerning FTIR spectral analysis of weakly interacting blend systems are found in the literature. PAS, which features carbonyl groups, is an ideal model polymer for a wide variety of such studies. In our previous reports,[24−27] we have noted that the wavenumber of the PAS carbonyl group in FTIR spectra depends on the relative interaction strength of the units in the PAS polymer main chain. For example, the signal of the carbonyl group of PAS shifts to higher wavenumber upon incorporating an inert diluent (i.e., a nonpolar group), such as when acetoxystyrene is copolymerized with styrene to form poly(styrene-*co*-acetoxystyrene) (PS-*co*-PAS).[24] The carbonyl stretching frequency of PAS that is blended with phenolic resin is split into two bands, which correspond to the free and the hydrogen-bonded carbonyl groups, with the latter at a lower wavenumber.[27] In this study, the weak interactions of the binary PAS/PEO blend system were investigated by FTIR spectroscopy and compared with similar systems previously reported.

[†] National Chiao Tung University.
[‡] National Ping-Tung University of Science and Technology.
* To whom corresponding should be addressed: Tel 886-3-5727077; Fax 886-3-5719507; e-mail changfc@cc.nctu.edu.tw.

10.1021/ma035417e CCC: $27.50
Published on Web 04/28/2004

The generalized two-dimensional (2D) IR correlation spectroscopy proposed by Noda[28−30] has been widely applied in polymer science in recent years. This novel method treats spectral fluctuations as a function of time, temperature, pressure, and composition and allows the specific interactions between polymer chains to be investigated. 2D IR correlation spectroscopy can identify different intra- and intermolecular interactions through selected bands from the one-dimensional vibrational spectrum. In this study, we have used generalized 2D IR correlation spectroscopy to explore the weak hydrogen-bonding interaction in blends of PEO and PAS.

Furthermore, the effects on spherulite growth rates in miscible binary blends of amorphous/crystalline polymers have attracted great interest.[31−38] Generally, a depression of the crystal growth rate of the crystallizable component is found upon addition of the amorphous component. The properties of crystallizable blends depend on the miscibility between their components and their resultant crystalline morphologies. In this paper, we emphasize the effect of miscibility on the spherulite growth behavior relative to pure PEO.

Experimental Section

Materials. The polymer used in this study, poly(acetoxystyrene), was synthesized by free radical polymerization in benzene at 80 °C under a nitrogen atmosphere using azobis(isobutyronitrile) (AIBN) initiator. The product was purified by dissolving in benzene, reprecipitating from cyclohexane, and then drying in a vacuum oven at 80 °C for 12 h. The molar mass and polydispersity were determined at room temperature by GPC using tetrahydrofuran (THF) as the mobile phase and gave M_n = 21 500 g/mol and M_w = 28 000 g/mol. The poly(ethylene oxide) (PEO) having M_n = 20 000 g/mol was obtained from Aldrich.

Preparations of Blends. Solution blending of PAS/PEO blends with various compositions was carried out in THF containing a total polymer content of 5 wt %. The polymer blend solution was stirred for 6−8 h, and then the solution was evaporated slowly at room temperature for 1 day. The film of the blend was then dried at 50 °C for 2 days to remove any residual solvent.

Characterizations. The melting and crystallization behavior and the glass transition temperatures of the polymer blends were studied by DSC using a Du-Pont DSC-9000. The glass transition temperature was determined using a scan rate of 20 °C/min over the temperature range 30−150 °C. Approximately 5−10 mg of each blend was weighed and sealed in an aluminum pan. The sample was quickly cooled to −100 °C from the melt of the first scan and then scanned between −100 and 250 °C at 20 °C/min. The glass transition temperature is at the midpoint of the specific heat increment. DSC was also employed to study the isothermal crystallization by rapid cooling to the crystallization temperature (T_c) from the melt at 80 °C for 10 min and then maintaining the sample at T_c for 12 h. After the isothermal crystallization was complete, the sample was cooled to 0 °C and then heated to 100 °C at a heating rate of 10 °C/min to measure the melting temperature (T_m). Infrared spectra of polymer blend films were obtained by the conventional KBr disk method. A THF solution containing the blend was cast onto a KBr disk and dried under conditions similar to those used in the bulk preparation. The film used in this study was thin enough to obey the Beer−Lambert law. FTIR spectra were recorded on a Nicolet Avatar 320 FT-IR spectrophotometer by collecting 32 scans at a resolution of 1 cm^{-1}. For solution samples, an adequately sealed cell with NaCl windows and a sample thickness of 0.05 mm was used to obey the Beer−Lambert law.

2D IR correlation analysis was conducted using "Vector 3D" software (Bruker Instrument Co.). All of the spectra subjected to the 2D correlation analyses were normalized and classified into two sets: A and B. The spectra in set A are, in order, pure PAS, PAS/PEO = 90/10, PAS/PEO = 80/20, PAS/PEO = 70/30, and PAS/PEO = 60/40. Those in set B are, in order, PAS/PEO = 50/50, PAS/PEO = 40/60, PAS/PEO = 30/70, PAS/PEO = 20/80, and pure PEO. Shaded regions indicate the negative intensity of autopeaks or cross-peaks in the 2D-correlation spectrum; unshaded regions indicate positive. The synchronous 2D IR spectrum was used to study the specific interaction between PEO and PAS in the blends, while the asynchronous 2D IR spectrum was used to separate the bands of pure PEO from those of the spectra of PAS/PEO blends. The spherulite growth rate was determined by using a polarized light microscope (Olympus Limited Co., Japan) equipped with a heating stage (Mettler- FP90); photographs were taken with a CCD camera. Each sample was sandwiched between two thin glass slides, melted for 10 min on a hot stage at 80 °C, and then transferred as quickly as possible onto another hot stage preheated to the desired crystallization temperature (T_c). The sample was crystallized isothermally at a given T_c to monitor the growth of the spherulite as a function of time. The radial growth rate of the PEO spherulite was calculated as the slope of the line obtained from a plot of the spherulitic radius vs time.

Results and Discussion

Miscibility and Melting Behavior. Figure 1 shows the DSC thermograms of PAS/PEO blends and indicates that pure PAS displays one T_g at 122 °C and that the melting temperature of pure PEO is 70 °C. The value of T_g of the PAS component shifts to lower temperature as the PEO content in the blend is increased. Meanwhile, the melting temperature of the PEO component in the blend decreases with increasing PAS content. A melting temperature depression is characteristic of a miscible polymer blend in a melting state in which a thermodynamic equilibrium is achieved. Table 1 summarizes the thermal properties of PAS, PEO, and their blends. All PAS/PEO blends show only one single glass transition temperature at all blend compositions. A single value of T_g strongly suggests that these two components are fully miscible in the amorphous phase. Figure 2 shows the dependence of the value of T_g on the composition of the miscible PAS/PEO blends. Over the years, many equations have been suggested for predicting the variation of the glass transition temperature of a miscible blend as a function of composition. The most popular equation for a system with strong intermolecular interactions is the Kwei equation,[39] but a more suitable equation for weakly interacting system is the Gordon−Taylor equation:[40]

$$T_g = (w_1 T_{g1} + k w_2 T_{g2})/(w_1 + k w_2) \qquad (1)$$

where w_1 and w_2 are weight fractions of the components, T_{g1} and T_{g2} represent the corresponding glass transition temperatures, and k is the fitting constant. We obtained a value of k = 0.14 by a nonlinear least squares "best fit" analysis of the equation. For comparison, this value is closed to that k was 0.145−0.45 for the poly(phenyl methacrylate)/PEO blend,[41] and k was ∼0.17 for the poly(benzyl methacrylate)/PEO blend.[42] This low value of k suggests that the intermolecular interactions in this system is not strong. The deviation of experimental T_g from the Gordon−Taylor equation at higher PEO content is due to the crystallization of PEO in the blends during quenching. This phenomenon shows not only the crystallization of PEO in the blends can change the amorphous phase but also the crystal of PEO is able to act as a physical cross-linking point that may hinder the molecular mobility of amorphous phase.

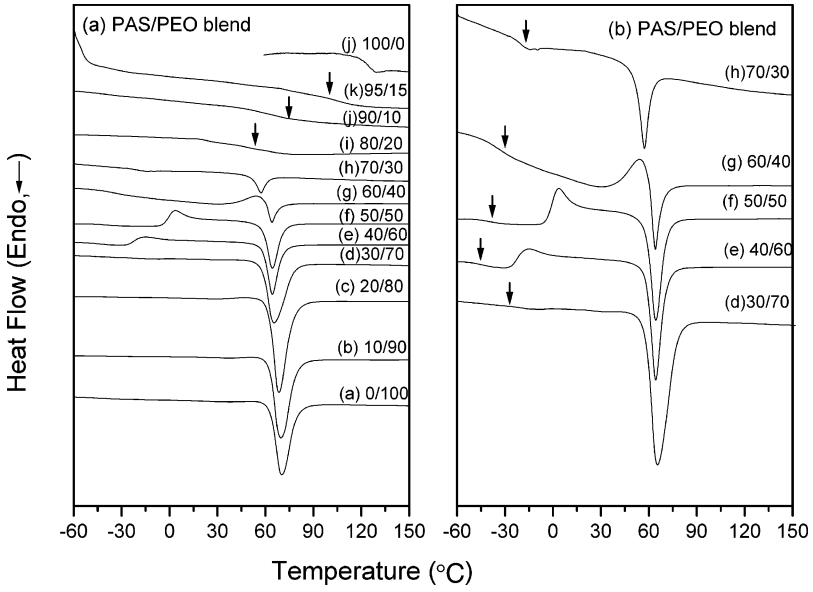

Figure 1. (a) DSC scans of PAS/PEO blends having different compositions. (b) Scale expanded the compositions of (a).

Table 1. Thermal Properties of PAS/PEO Blends

PAS/PEO	T_g (°C)	T_m (°C)	ΔH_f (J/g)	T_c (°C)	ΔH_c (J/g)
100/0	122.1				
95/5	98.0				
90/10	69.0				
85/15	32.0				
80/20	13.2				
75/25	−13.2				
70/30	−19.1	58.3	10.6		
60/40	−32.1	64.1	20.2	54.9	4.5
50/50	−38.6	64.3	70.2	3.6	38.8
40/60	−45.3	64.4	111.8	−15.2	48.5
30/70	−19.0	67.4	120.5		
25/75		67.9	138.0		
20/80		68.5	149.4		
15/85		69.2	152.0		
10/90		69.7	171.6		
5/95		70.2	174.0		
0/100	−62.0	70.5	175.7		

In addition, the extent of the melting point depression of a crystalline polymer blended with an amorphous polymer can provide important information regarding their miscibility and their polymer−polymer interaction parameter. The temperature reduction is caused not only by morphological effects but also for thermodynamic reasons. From the thermodynamic consideration, thermodynamic properties of the crystalline component in the amorphous phase can be determined. When two polymers are miscible in the molten state, the chemical potential of the crystallizable polymer is decreased due to the addition of the second component. The method described by Hoffman and Weeks[43] was adopted to determine the equilibrium temperature for PAS/PEO blends. Figure 3 displays the Hoffman−Weeks plots to obtain the equilibrium melting temperatures of pure PEO (T_m^0) and the PEO component in various PAS/PEO blends (T_{m2}^0). The equilibrium melting temperature of the PEO component decreases upon increasing the weight fraction of PAS because of the decrease in the chemical potential resulting from the addition of the second component. The data obtained in this study were analyzed on the basis of the Flory−Huggins theory[44] in which the melting

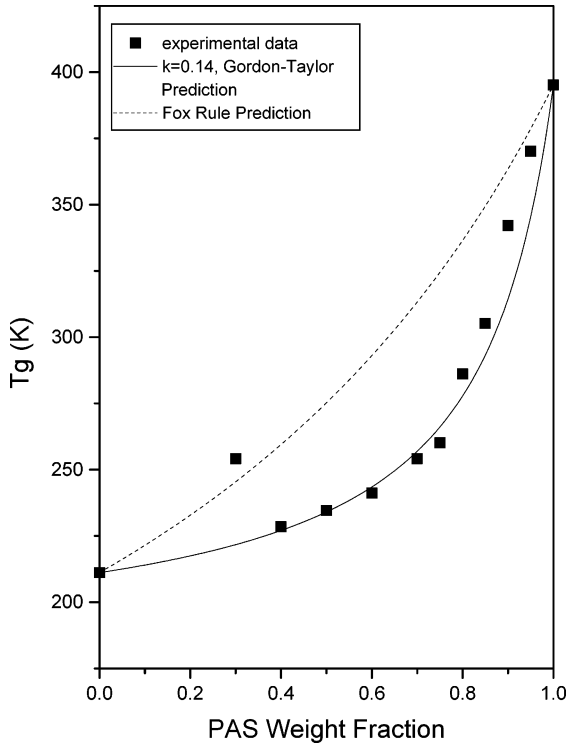

Figure 2. Plots of T_g vs composition based on (■) experimental data, (- - -) the Fox rule, and (—) the Gordon−Taylor equation.

point depression is given by eq 2:

$$\frac{1}{T_m^0} - \frac{1}{T_{m2}^0} = \frac{-R}{\Delta H_{2u}} \frac{V_{2u}}{V_{1u}} \chi_{12} \phi_1^{\,2} \qquad (2)$$

The terms T_m^0 and T_{m2}^0 denote the equilibrium melting points of the crystallizable component alone and in the blend, respectively. The terms V_{2u} and V_{1u} are the molar volumes of the repeating units of the blend components; R is the universal gas constant. The term ΔH_{2u} is the heat of fusion of the perfectly crystallized polymer per mole of repeat unit; the subscript 1 represents the amorphous polymer, and the subscript 2 represents the

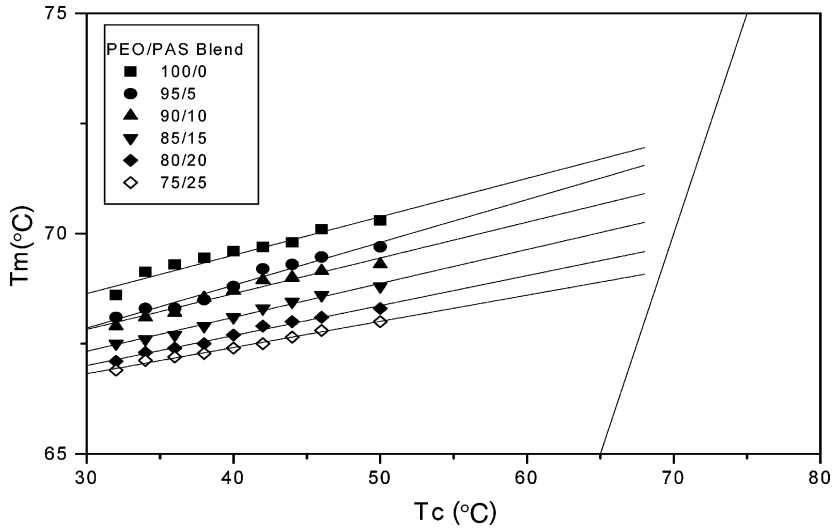

Figure 3. Hoffman−Weeks plots for PAS/PEO blends.

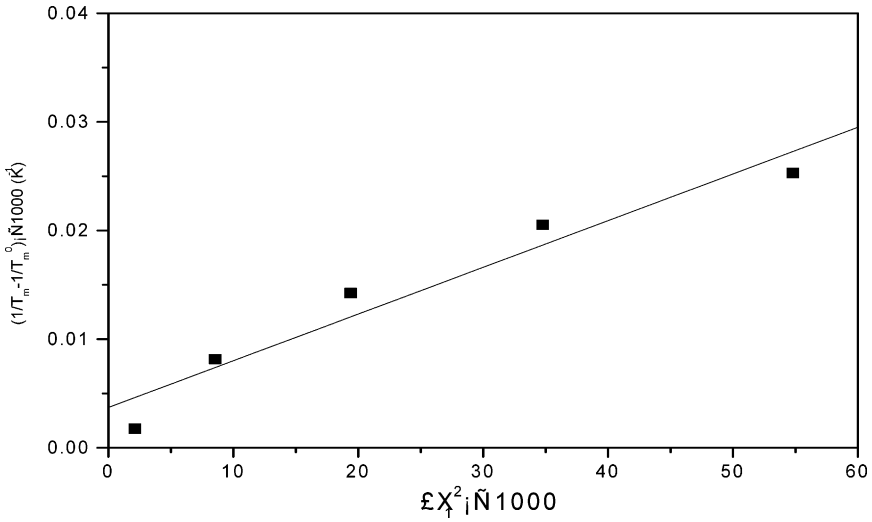

Figure 4. Plots of the depression of the equilibrium melting temperature vs the square of the volume of fraction of PAS.

crystalline polymer. ϕ is the volume fraction of the component in the blend, and χ_{12} is the polymer−polymer interaction parameter. As shown in Figure 4, the melting point depression of the PAS/PEO blend increases linearly with the volume fraction of the amorphous component (ϕ_1). The weight fraction can be converted into the volume fraction by using the molar volume of monomeric units as determined by a group contribution method.[1] The interaction parameter χ_{12} also can be written as

$$\chi_{12} = \frac{B_{12}V_{1u}}{RT} \tag{3}$$

where B_{12} denotes the interaction energy density between blend components. In this work, we calculate a value of $\chi_{12} = -1.82 \pm 0.2$ from the slope of Figure 4 according to eq 2 based on $V_{2u} = 38.1$ cm^3/mol and $\Delta H_{2u} = 1980$ cal/mol[6] and $B_{12} = -6.64 \pm 0.8$ according to eq 3 based on $V_{1u} = 162.2$ cm^3/mol.[25] The negative values of χ_{12} and B_{12} are consistent with a miscible system. This value is smaller than the strong hydrogen-bonding systems such as PVPh-*co*-PMMA/PEO ($B_{12} = -29.23$)[9] and phenolic/PCL blends ($B_{12} = -12.51$).[45] Therefore, this lower value suggests that the intermolecular interactions in this blend system is not strong.

Analyses by Fourier Transform Infrared Spectroscopy. Infrared spectroscopy is a highly effective means of investigating the specific interactions between polymers. It can be used to study, both qualitatively and quantitatively, the mechanism of interpolymer miscibility through the formation of hydrogen-bonding or dipole−dipole interactions. Figure 5 shows infrared spectra of various PAS/PEO blend compositions recorded at room temperature in the region 600−3600 cm^{-1}. Table 2 lists detailed peak assignments for PEO and PAS. Broader absorption peaks were found for ether stretching at ca. 1100 cm^{-1} in spectra of the blends relative to that of the pure PEO homopolymer.

Next we examined the carbonyl stretching region of the PAS/PEO blends. Figure 6 shows scale-expanded IR spectra of neat PAS and various PAS/PEO blends recorded in the region 1680−1800 cm^{-1} at room temperature. The absorption at 1760 cm^{-1} is assigned to the free carbonyl group of the PAS. Clearly, the half-width of this signal increases upon blending with PEO; the largest such half-width occurs for the blends containing PEO content of 20 wt %. The narrower half-width at higher PEO content can be explained by the fact that these blend systems possess a crystalline phase. Consequently, the intermolecular interaction between the PAS and PEO segment tends to decrease

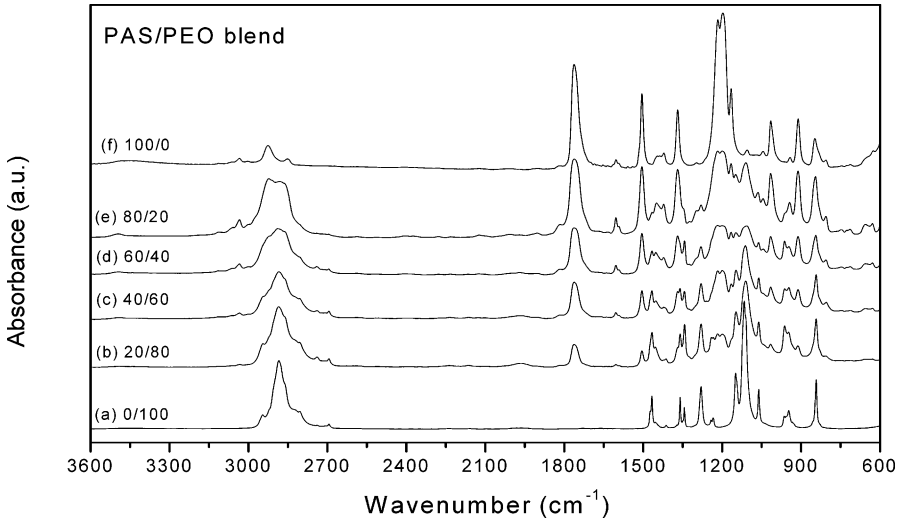

Figure 5. FTIR spectra of PAS/PEO blends in the 600−3600 cm^{-1} region recorded at room temperature.

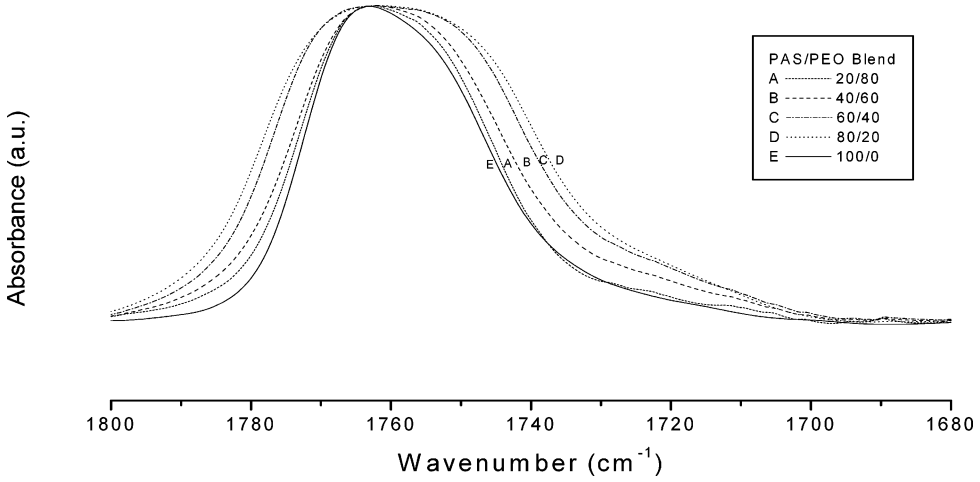

Figure 6. FTIR spectra of PAS/PEO blends in the 1680−1800 cm^{-1} region recorded at room temperature.

Table 2. Frequencies and Peak Assignments of the FTIR Bands of PAS and PEO

PEO (cm^{-1})	PAS (cm^{-1})	assignments
	3037	benzene ring CH stretching
	2924	CH_2 stretching
2884		CH_2 stretching
	1763	C═O stretching
	1603	C−C ring in plane strength
1467		CH_2 bending
	1455, 1421	asymmetric CH_2 stretching
	1368	symmetric carboxylate stretching
1360		CH_2 wagging (crystalline)
1343		CH_2 wagging (crystalline)
1280		CH_2 twist
1234		CH_2 twist
	1215	acetate stretching
	1193	acetate asymmetric stretching
1149		C−O−C stretching, C−C stretching
1116		C−O−C stretching
1060		C−O−C stretching, CH_2 rocking
	1015	C−O stretching
962		CH_2 rocking
946		CH_2 rocking, C−O−C stretching
	911	CH_2 out-of-line bending
	846	CH_2 out-of-line bending
842		CH_2 rocking

with the increase of PEO content due to reduced chain mobility in the PEO crystalline phase. However, it is also clear that intermolecular interactions occur between the PAS and the PEO because of the significant

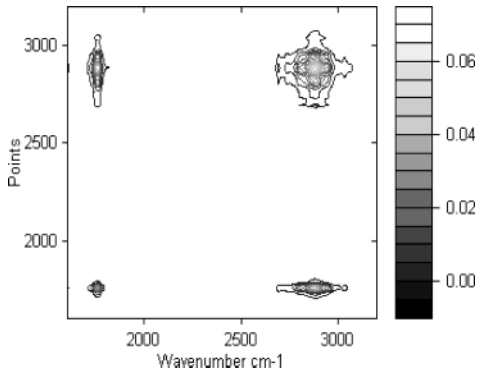

Figure 7. Synchronous 2D correlation map of set A in the region 1600−3200 cm^{-1}.

changes to the carbonyl group of the PAS. To confirm that the intermolecular interaction exists between the PAS and the PEO polymers, two-dimensional infrared spectra were obtained.

Figure 7 shows the synchronous 2D correlation maps of set A in the range 1600−3200 cm^{-1}. Bands in this spectral range corresponding to PAS appear at 3037, 2924, 2849, and 1760 cm^{-1}, which are due to C−H aromatic, CH, CH_2, and carbonyl (C═O) stretching vibrations, respectively. However, the only signal of pure PEO appears at 2884 cm^{-1}, which arises from CH_2 stretching vibrations. Clearly, two positive cross-peaks

Scheme 1. Model of the Interaction between PAS and PEO Polymer Chains

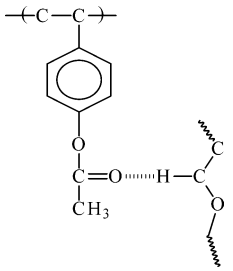

are visible in Figure 7, which indicate that the carbonyl group of PAS interacts not only with the methylene (CH_2) segment of PEO through weak C−H···O hydrogen bonding but also with the methylene segment of PEO because of the contribution from the same chain. In addition, Figure 8a,b displays the asynchronous 2D correlation maps of the spectra of set A in the range 1600−3200 cm^{-1}, which show that the intensities of the two cross-peaks have opposite signs. To summarize these results, we conclude that PAS and PEO are reoriented with respect to another at the molecular level because the carbonyl groups of PAS interact with the methylene segments of PEO, as indicated in Scheme 1. The rate at which the CH_2 units of PAS are reoriented varies with the PEO content, however, which indicates that two microenvironment motions exist in this binary blend system.

Figure 9 displays FTIR spectra highlighting the carbonyl stretching peak in the range from 1680 to 1800 cm^{-1} recorded at room temperature with a 0.01 M concentration of *p*-tolyl acetate (TAc, a model compound for PAS) in cyclohexane, PS55-*co*-PAS45 copolymer, pure PAS, the PAS/PEO = 20/80 blend, and the phenolic/PAS = 40/60 blend. Clearly, the wavenumbers and half-widths of the carbonyl signal depend significantly on the dipole−dipole or hydrogen-bonding interaction on the molecules or polymer chains. Compared with pure PAS, the carbonyl band of TAc in cyclohexane is thinner

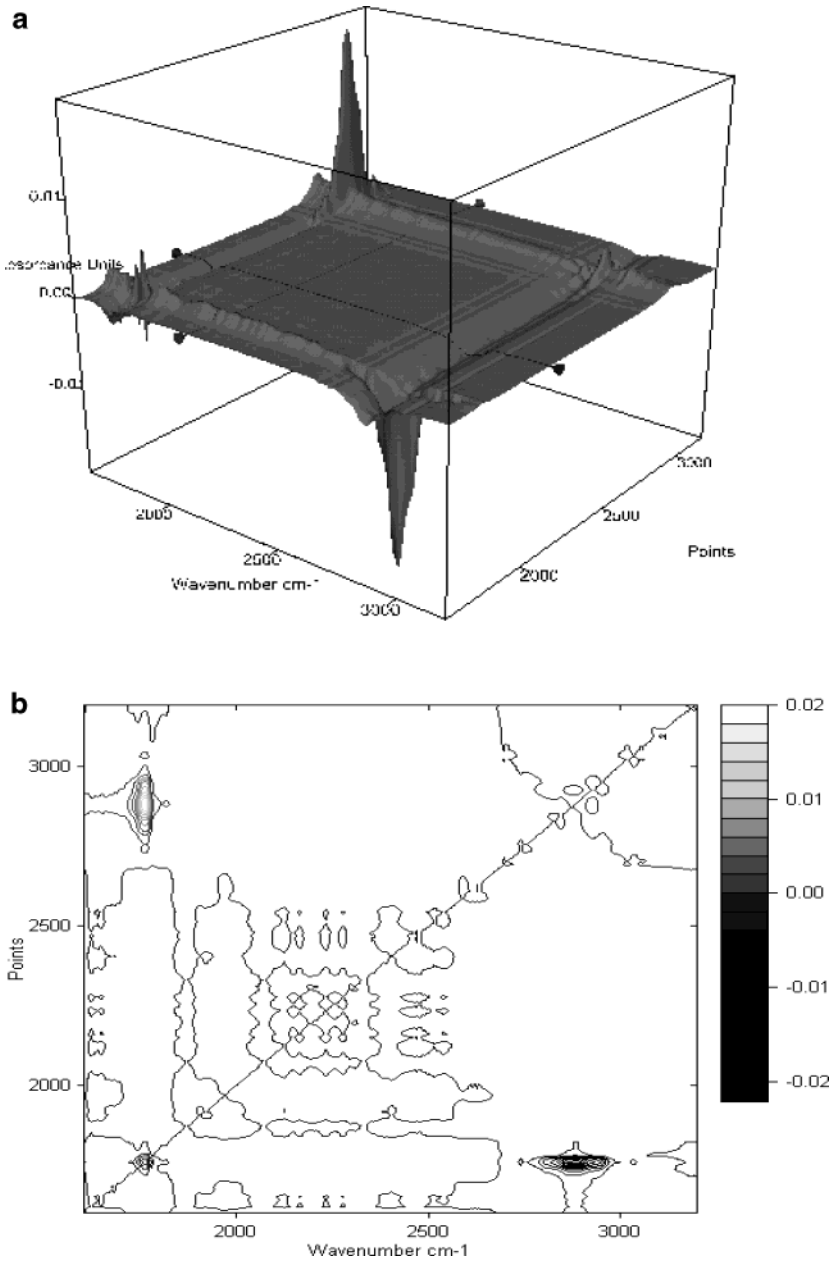

Figure 8. Asynchronous 2D correlation map of set A in the region 1600−3200 cm^{-1}.

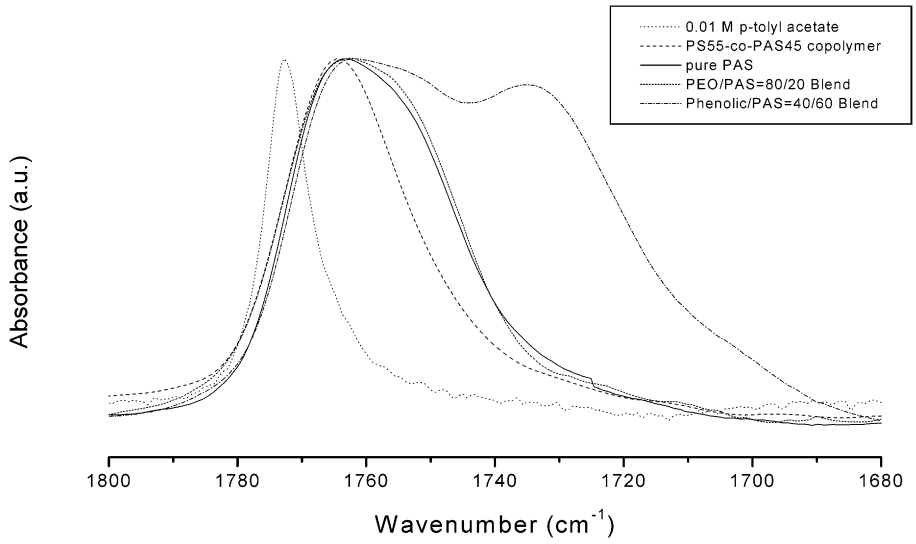

Figure 9. FTIR spectra recorded at room temperature of 0.01 M *p*-tolyl acetate in cyclohexane, PS55-*co*-PAS45, pure PAS, the PAS/PEO = 20/80 blend, and the phenolic/PAS = 40/60 blend showing the carbonyl stretching peaks in the 1680−1800 cm^{-1}.

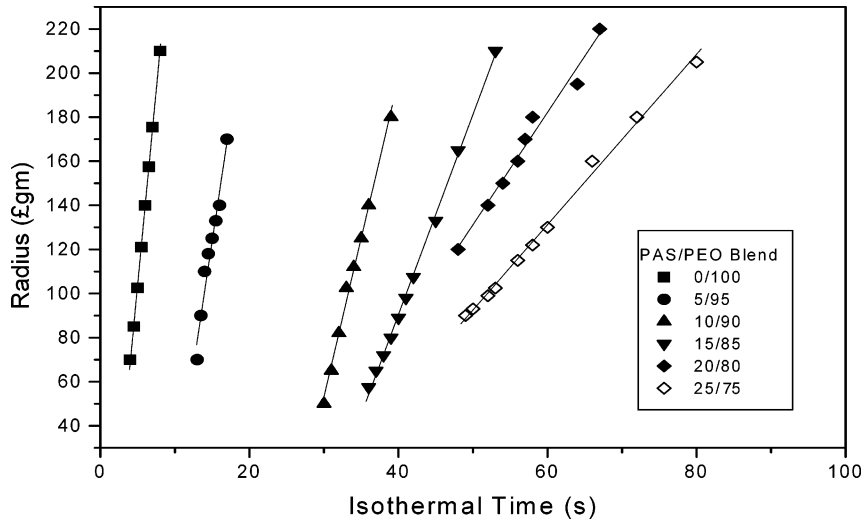

Figure 10. Radii of spherulites as a function of time at 46 °C for various PAS/PEO blend compositions.

and is shifted to a higher wavenumber because of the lower probability of carbonyl−carbonyl dipole interactions. At the same time, the carbonyl group of PAS also shifts to a higher wavenumber upon copolymerization with styrene to produce PAS-*co*-PS, indicating that the number of carbonyl−carbonyl interactions decreases with the incorporation of the inert diluent segment (styrene units). In addition, the carbonyl stretching frequency of PAS blended with phenolic resin is split into two bands that correspond to free and hydrogen-bonded carbonyl groups, the latter at lower wavenumber (1735 cm^{-1}). When blended with PEO, however, the only effect on the signal of the PAS carbonyl groups is that its half-width increases. The observed effects of the intermolecular interactions is in the order phenolic/PAS blend > PAS/PEO blend > pure PAS polymer > PS-*co*-PAS copolymer. This result indicates that the strength of the intermolecular hydrogen bonding in the phenolic/PAS blend is stronger than that of the weak hydrogen-bonding interactions of the PAS/PEO blend.

Spherulite Growth Kinetics. The dimensions of the crystallites are very sensitive to the crystallization temperature and time. For brevity, Figure 10 displays plots of the spherulite radius vs time of various PAS/PEO compositions crystallized at 46 °C; the solid lines represent the best least-squares fit to the data. It is clear that there is a linear increase in the radius with time until the spherulite impinges on others. The slope of the line decreases with increasing PAS content, as displayed by Figure 10. Figure 11 presents plots of the crystallization rate (*G*) as a function of the crystallization temperature (T_c) for pure PEO and various PAS/PEO blends; the spherulite growth rate decreases with increasing PAS content at a given value of T_c. The presence in the blend of amorphous PAS having a high value of T_g decreases the rate of PEO crystallization significantly.

We adopted the Lauritzen−Hoffman model to analyze the spherulite crystallization behavior of PAS/PEO blends.[46] The equation is

$$G = G_0 \exp\left[\frac{-U^*}{R(T - T_\infty)}\right] \exp\left[\frac{-K_g}{f\,T\Delta T}\right] \qquad (4)$$

where G_0 is the front factor, U^* is the activation energy for segment diffusion to the site of crystallization, R is the gas constant, T_∞ is the hypothetical temperature below which all viscous flow ceases, K_g is the nucleation parameter, ΔT is the degree of supercooling defined as

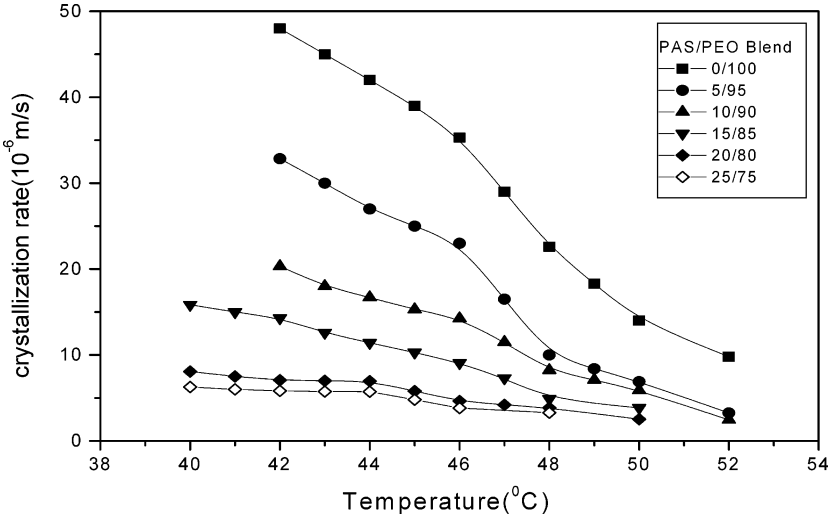

Figure 11. Radial growth rate (G) as a function of T_c for PAS/PEO blends.

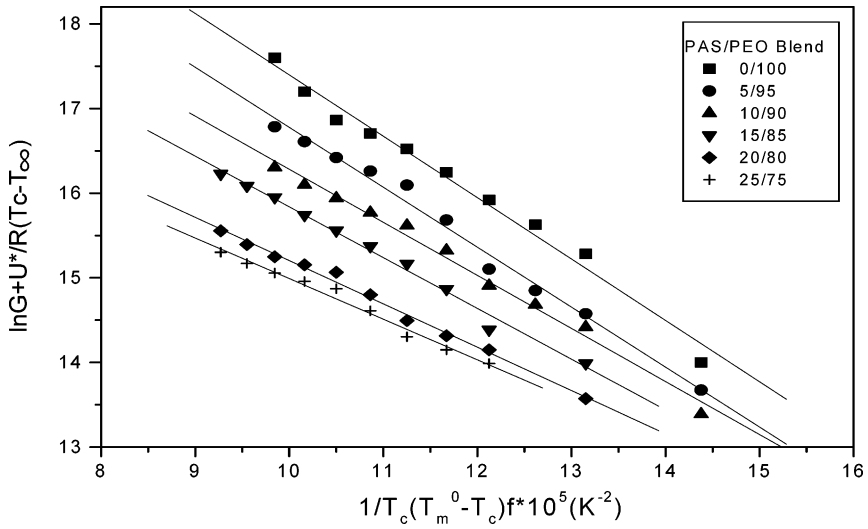

Figure 12. Kinetics analysis of the crystallization rate constant data employing the WLF constants.

$T_m^0 - T_c$, and f is a correction factor given as $2T_c/(T_m^0 + T_c)$. We emphasize that the parameters U^* and T_∞ are treated as variables to maximize the quality of the fit of the data to eq 4. In this study, we used the Williams−Landel−Ferry (WLF) values of $U^* = 4120$ cal/mol and $T_\infty = T_g - 51.6$.[47] The nucleation parameter K_g is given by[47−49]

$$K_g = \frac{nb\sigma\sigma_e T_m^0}{\Delta h_f k_B} \tag{5}$$

where b is the thickness of a monomolecular layer; σ is the lateral surface free energy, σ_e is the surface free energy of chain folding, Δh_f is the heat of fusion per unit volume, T_m^0 is the equilibrium melting temperature, and k_B is Boltzmann's constant. Typically, values have been employed of $n = 4$ in regimes I and III and $n = 2$ in regime II. It is often most convenient to rearrange eq 4 as eq 6:

$$\ln G + \frac{U^*}{R(T - T_\infty)} = \ln G_0 - \frac{K_g}{T(\Delta T)f} \tag{6}$$

to view the growth rate data in the form of a plot of the left-hand side of eq 6 vs $1/T_c(\Delta T)f$, with a slope $= -K_g$.

Table 3. Comparisons of the Nucleation Constants and Surface Free Energies of PAS/PEO Blends

compositions (PAS/PEO blends)	K_g (III) $\times 10^{-4}$ (deg^2)	σ_e (erg/cm^2)
0/100	7.7	35.7
5/95	7.1	32.6
10/90	6.3	28.8
15/85	6.0	27.5
20/80	5.1	23.5
25/75	4.8	22.1

Figure 12 shows such plots according to eq 6; the values of K_g obtained are summarized in Table 3. In this study, the regime is assigned to be regime III at about 40−50 °C.[50] The derived values of K_g can be used to calculate the surface free energy of chain folding (σ_e) and the work of chain folding (q) for PEO. Using the thickness $b = 0.465$ nm^2, $T_m^0 = 72.9$ °C, and $\Delta h_f = 2.13 \times 10^9$ erg/cm^3 as previously determined,[51] the lateral surface free energy σ can be estimated by the Thomas−Stavely relationship:[52]

$$\sigma = \alpha b_0(\Delta h_f) \tag{7}$$

where α is an empirical constant which is usually assumed to be 0.1 for vinyl polymers and $\alpha = 0.25$ for

high melting polyesters.[32] For a low melting point polyether, such as PEO, which has a long run of CH_2 groups like PE, a value of 0.1 is recommended. The obtained value of $\sigma_e = 35.7$ erg/cm^2 for pure PEO agrees well with previously reported.[48] The values of K_g(III) and σ_e for various blend compositions are also listed in Table 3. Both values decrease upon increasing the PAS content, which indicates that the crystallization ability of PEO in the blend increases with increasing PAS content. The same trend in the surface free energy of chain folding was also observed in the PBzMA/PEO blend system: it decreases with increasing PBzMA content in that blend.[42] This result indicates that the amorphous component of PAS reduces the surface free energy of chain folding and provides the driving force for crystallization of PEO, which is consistent with our previous study.[53] The relative weakly interacting blends such as the SAN/PCL, PVAc/PEO, PVAc/PHB, and phenoxy/PCL blends would have lower surface free energy of chain folding than that of pure crystallizable polymer.[53] This phenomenon can be predicted by a recent theoretical model that a miscible blend of polymers with a relatively large difference in values of T_g that exhibits weak intermolecular interactions will display two dynamic microenvironments.[54] One is near the mean blend mobility, and the other is close to that of the component with the lower value of T_g. In the 2D FTIR analysis described above, two cross-peaks were observed having opposite signs of their intensities, which indicates that the microphase separation occurs because of two different motions in this binary PAS/PEO blend. The amorphous component of PAS may play the role of a nucleation agent by reducing the surface free energy of chain folding and provides the driving force for crystallization of PEO. The surface free energy of chain folding is lower than pure PEO would induce the smaller crystalline thickness;[53] thus, this result is important in blends where melting depression is very small.

Conclusions

The binary PAS/PEO blend system is fully miscible as indicated by a single glass transition temperature over a full range of compositions as a result of the formation of weak hydrogen-bonding interactions between the carbonyl group of PAS and the methylene groups of PEO. In addition, a negative polymer−polymer interaction parameter was calculated from the melting depression of PEO, using the Flory−Huggins equation. Two-dimensional FTIR spectroscopy studies provide positive evidence for the intermolecular interaction between the PAS carbonyl group and the PEO methylene group. The crystallization behavior of PEO from the melt is strongly influenced by the composition and the crystallization temperature. The addition of a PAS component into PEO causes a depression in its spherulite growth rate. The values of the nucleation constant and the surface free energy of chain folding of PEO decrease with increasing PAS content, which indicates that the crystallization ability of PEO in blends increases with increasing PAS content.

Acknowledgment. The authors thank the National Science Council, Taiwan, Republic of China, for financially supporting this research under Contract NSC-92-2216-E-009-018.

References and Notes

(1) Coleman, M. M.; Graf, J. F.; Painter, P. C. *Specific Interactions and the Miscibility of Polymer Blends*; Technomic Publishing: Lancaster, PA, 1991.
(2) Espi, E.; Iruin, J. J. *Macromolecules* **1991**, *24*, 6458.
(3) Zheng, S.; Al, S.; Guo, Q. *J. Polym. Sci., Polym. Phys. Ed.* **2003**, *41*, 466.
(4) Jiang, M.; Li, M.; Zhou, H. *Adv. Polym. Sci.* **1999**, *146*, 121.
(5) Tsuchida, E.; Abe, K. *Adv. Polym. Sci.* **1982**, *45*, 1.
(6) Jo, W. H.; Lee, S. C. *Macromolecules* **1990**, *23*, 2261.
(7) Akiba, I.; Ohba, Y.; Akiyama, S. *Macromolecules* **1999**, *32*, 1175.
(8) Sawatari, C.; Kondo, T. *Macromolecules* **1999**, *32*, 1949.
(9) Kuo, S. W.; Chang, F. C. *Macromolecules* **2001**, *34*, 4089.
(10) Jack, K. S.; Whittaker, A. K. *Macromolecules* **1997**, *30*, 3560.
(11) Wu, H. D.; Chu, P. P.; Ma, C. C. M.; Chang, F. C. *Macromolecules* **1999**, *32*, 3097.
(12) Kuo, S. W.; Lin, C. L.; Chang, F. C. *Macromolecules* **2002**, *35*, 278.
(13) Zawada, J. A.; Ylitalo, C. M.; Fuller, G. G.; Colby, R. H.; Long, T. E. *Macromolecules* **1992**, *25*, 2896.
(14) Wastlund, C.; Maurer, F. H. J. *Macromolecules* **1997**, *30*, 5870.
(15) Chen, X.; An, L.; Yin, J.; Sun, Z. *Macromolecules* **1999**, *32*, 5905.
(16) Kalfoglou, N. K. *J. Polym. Sci., Polym. Phys. Ed.* **1982**, *20*, 1295.
(17) Feldstein, M. M.; Shandryuk, G. A.; Kuptsov, S. A.; Plate, N. A. *Polymer* **2000**, *41*, 5327.
(18) Cortazar, M. M.; Calahorra, M. E.; Guzman, G. M. *Eur. Polym. J.* **1982**, *18*, 165.
(19) Li, X.; Hsu, S. L. *J. Polym. Sci., Polym. Phys. Ed.* **1984**, *22*, 1331.
(20) Calahorra, M. E.; Cortazar, M. M.; Guzman, G. M. *Polymer* **1982**, *23*, 1322.
(21) Ito, H.; Russell, T. P.; Wignall, G. D. *Macromolecules* **1987**, *20*, 2213.
(22) Ramana, R. G.; Castiglioni, C.; Zerbi, G.; Martuscelli, E. *Polymer* **1985**, *26*, 811.
(23) Coleman, M. M.; Painter, P. C. *Prog. Polym. Sci.* **1995**, *20*, 1.
(24) Kuo, S. W.; Chang, F. C. *Polymer* **2001**, *43*, 9843.
(25) Kuo, S. W.; Liu, W. P.; Chang, F. C. *Macromolecules* **2003**, *36*, 5165.
(26) Kuo, S. W.; Chang, F. C. *Polymer* **2003**, *44*, 3021.
(27) Kuo, S. W.; Chang, F. C. *Macromol. Chem. Phys.* **2002**, *203*, 868.
(28) Noda, I. *J. Am. Chem. Soc.* **1989**, *111*, 8116.
(29) Ren, Y.; Murakami, T.; Nishioka, T.; Nakashima, K.; Noda, I.; Ozaki, Y. *Macromolecules* **1999**, *32*, 6307.
(30) Makashima, K.; Ren, Y.; Nishioka, T.; Tsubahara, N.; Noda, I.; Ozaki, Y. *J. Phys. Chem. B* **1999**, *103*, 6704.
(31) Wang, T. T.; Nishi, T. *Macromolecules* **1977**, *10*, 421.
(32) Alfonso, G. C.; Russell, T. P. *Macromolecules* **1986**, *19*, 1143.
(33) Russell, T. P.; Ito, H.; Wignall, G. D. *Macromolecules* **1988**, *21*, 1073.
(34) Crevecoeur, G.; Grenninckx, G. *Macromolecules* **1991**, *24*, 1190.
(35) Runt, J.; Miley, D. M.; Zhang, X.; Gallagher, K. P.; McFeaters, K.; Fishburn, J. *Macromolecules* **1992**, *25*, 1929.
(36) Zemel, I. S.; Roland, C. M. *Polymer* **1992**, *33*, 3427.
(37) Runt, J. In *Polymer Blends*; Paul, D. R., Ed.; John Wiley & Sons: New York, 2000; Vol. 1.
(38) Talibuddin, S.; Wu, L.; Runt, J.; Lin, J. S. *Macromolecules* **1996**, *29*, 7527.
(39) Kwei, T. K. *J. Polym. Sci., Polym. Lett. Ed.* **1984**, *22*, 307.
(40) Gordon, M.; Taylor, J. S. *J. Appl. Chem.* **1952**, *2*, 493.
(41) Woo, E. M.; Mandal, T. K.; Chang, L. L.; Lee, S. C. *Polymer* **2000**, *41*, 6663.
(42) Mandal, T. K.; Kuo, J. F.; Woo, E. M. *J. Polym. Sci., Polym. Phys. Ed.* **2000**, *38*, 562.
(43) Hoffman, J. D.; Weeks, J. J. *J. Chem. Phys.* **1965**, *42*, 4301.
(44) Flory, P. J. *Principles of Polymer Chemistry*; Cornell University Press: Ithaca, NY, 1953.
(45) Kuo, S. W.; Chang, F. C. *Macromol. Chem. Phys.* **2001**, *202*, 3112.
(46) Hoffman, J. D.; Davis, G. T.; Lauritzen, J. I., Jr., In *Treatise on Solid State Chemistry*; Hannay, N. B., Ed.; Plenum Press: New York, 1976; Vol. 3.
(47) Williams, M. L.; Landel, R. F.; Ferry, J. D. *J. Am. Chem. Soc.* **1975**, *77*, 3701.

(48) Hoffman, J. D. *Polymer* **1983**, *24*, 3.
(49) Phillips, P. J.; Rensch, G. J.; Taylor, K. D. *J. Polym. Sci., Polym. Phys. Ed.* **1987**, *25*, 1725.
(50) Cheng, S. Z. D.; Chen, J.; Janimak, J. J. *Polymer* **1990**, *31*, 1018.
(51) Godovsky, Y. K.; Slonimsky, G. L.; Garbar, N. M. *J. Polym. Sci., Part C* **1972**, *38*, 1.
(52) Thomas, D. G.; Staveley, L. A. K. *J. Chem. Soc.* **1952**, 4569.
(53) Kuo, S. W.; Chan, S. C.; Chang, F. C. *Macromolecules* **2003**, *36*, 6653.
(54) Kumar, S. K.; Colby, R. H.; Anastasiadis, H.; Fytas, G. *J. Chem. Phys.* **1996**, *105*, 3777.

MA035417E